ALFA: The MPIA/MPE* Adaptive Optics with a Laser for Astronomy Project

Stefan Hippler[a], Andreas Glindemann[a], Markus Kasper[a], Paul Kalas[a]
Ralf-Rainer Rohloff[a], Karl Wagner[a], Douglas P. Looze[b], and Wolfgang Hackenberg[c]

[a]Max-Planck-Institut für Astronomie, Königstuhl 17, 69117 Heidelberg, Germany

[b]University of Massachusetts, 211 Knowles Engineering Building, Amherst, MA 01003, U.S.A

[c]Max-Planck-Institut für extraterrestrische Physik, 85740 Garching, Germany

*Other MPE Project Members: see author list of paper 3353-94

ABSTRACT

The Max-Planck-Institutes for Astronomy (MPIA) and for Extraterrestrial Physics (MPE) have recently installed a laser guide star (LGS) adaptive optics (AO) system at the 3.5 m telescope on Calar Alto in Spain. The AO system consists of a Shack-Hartmann sensor, a deformable mirror with 97 actuators, and a wave-front processor that allows closed loop operations of up to 1200 Hz. As a first step we closed the high order AO loop on bright natural guide stars. As a second step we closed the AO loop on a 10th magnitude artificial LGS that is created in the mesospheric sodium layer by a 3.75 Watt dye laser. This paper describes ALFA's design, operation, and upgrade plans.

Keywords: adaptive optics, laser guide star, servo-loop control, modal correction

1. INTRODUCTION

ALFA (Adaptive optics with a Laser For Astronomy) will reach the end of its engineering and testing period in April 1998. It will be available as common user instrument on a shared risk basis starting in May 1998. After the summer semester 1998 it will be offered to the community as standard common user instrument for all near-infrared instrumentation available at the 3.5 m telescope on Calar Alto.

As reported in our previous papers[1–3] the performance goal for ALFA is to provide nearly diffraction-limited imaging at 2.2 µm ($0.16''$ FWHM for the 3.5 m mirror). Our aims are to achieve $\geq$ 50% Strehl ratio in the 2.2 µm band with good sky coverage, making the inclusion of an LGS system necessary.

2. THE LASER GUIDE STAR SYSTEM

The heart of the laser system is a 3.75 W dye ring laser pumped by a 25 W Argon ion laser. Both lasers are purchased from Coherent (Coherent 899 and Coherent INNOVA 200), and represent the highest CW output, off-the-shelf laser which is not pulsed. The output power is sufficient to produce an LGS with a magnitude of $m_V \approx 10$ (depending on meteorological conditions and zenith distance).

Pulse lasers with larger output power are also available but they entail several significant challenges. Due to the high output power in the pulses, security is a more difficult matter, the laser pulses have to be synchronized with the CCD camera, and saturation of the sodium layer can limit the maximum brightness of the artificial guide star.

The laser system is placed in the Coudé laboratory of the 3.5 m telescope building. The laser beam is guided backwards through the Coudé optical train to the side of the primary mirror and through additional optical elements into the focus of the launching telescope (Fig.1). The Coudé laboratory has the required power supply of 50 kW for the pump laser, and cooling water to dissipate heat. The cooling facility is more than one kilometre away from the telescope, avoiding problems with homemade seeing.

E-mail: hippler@mpia-hd.mpg.de, aglindem@eso.org, kasper@mpia-hd.mpg.de, kalas@mpia-hd.mpg.de
rohloff@mpia-hd.mpg.de, wagner@mpia-hd.mpg.de, looze@zonker.ecs.umass.edu, hacki@mpe.mpg.de
Present address of Andreas Glindemann: European Southern Observatory, Karl-Schwarzschild-Str. 2, 85748 Garching, Germany
ALFA homepage: http://www.mpia-hd.mpg.de/MPIA/Projects/ALFA

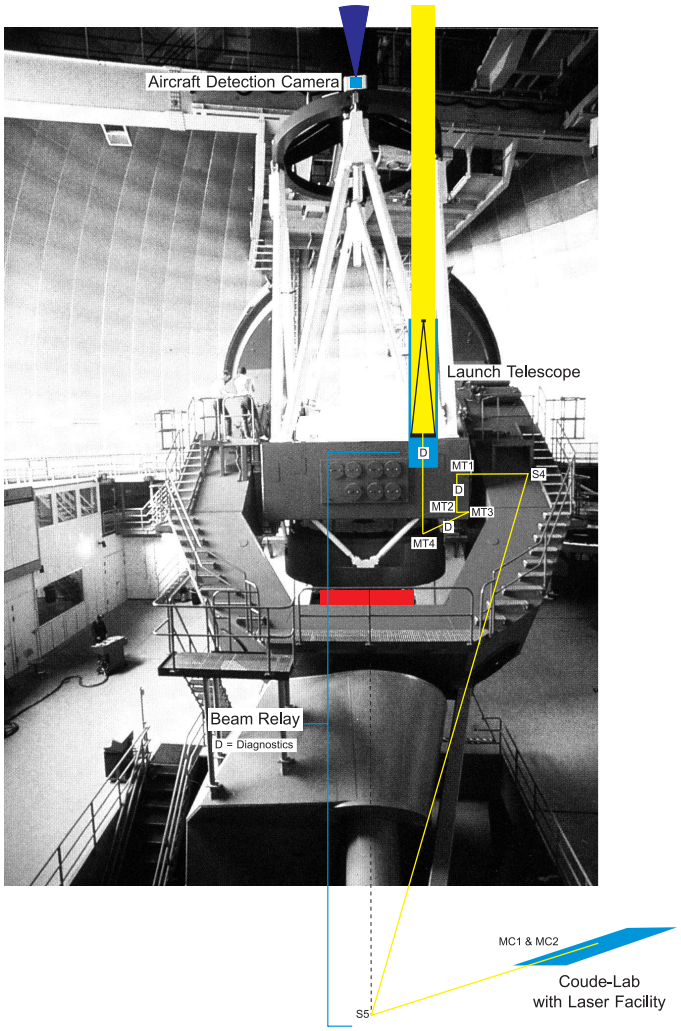

Figure 1. Schematics of the laser path on the 3.5 m telescope. The optical train from the Coudé focus to the mirror S4 is the standard Coudé path. The mirrors MT1 to MT4 are mounted additionally to transport the laser beam into the Cassegrain focus of the launching telescope with a diameter of 50 cm. The letter D denotes diagnostic elements in the optical path to ensure that the laser beam is held in the focus of the launching telescopes for all telescope positions. An aircraft detection system is mounted at the front ring of the telescope.

Guiding the laser beam from the Coudé focus to the focus of the launching telescope requires precise control over all the mirror positions since a small misalignment not only moves the position of the LGS, but it also deteriorates the illumination of the launch telescope pupil, decreasing the effective laser power. Thus, there are a number of CCD cameras and position sensitive detectors to monitor the position of the laser beam and a number of pilot lasers to control the position of the mirrors. This process is partially automated in a closed loop procedure. However, one should not underestimate the complexity of keeping the laser beam in a fixed position for all telescope angles.

Therefore, it seems very attractive to replace all the optical elements by a single optical fiber where the laser is fed into the fiber at the exit of the laser tube, and the end of the fiber is placed in the Cassegrain focus of the launching telescope to provide a point source. The main problem is the high energy density of about $1.4 \times 10^{11}\,\mathrm{W/m^2}$ at the tip of the fiber. Extreme care has to be taken to guarantee a clean surface. First experiments with an optical fiber at Calar Alto have shown that about 70% of the light can be coupled into the fiber (further results are presented in these proceedings by W. Hackenberg et al. and D. Bonaccini et al.). The efficiency of the mirror system is slightly higher but depends on the mirror surfaces.

The illuminated diameter of the launching telescope is chosen such that it is approximately $3\,r_0$ (approx. 30 cm), minimizing

the diameter of the instantaneous speckle image in the sodium layer. The energy density at the telescope exit is below the limits set by laser safety regulations; with less than $50\,W/m^2$ this is less than a standard He-Ne laser with 0.5 mW output power and a beam diameter of about 1 mm. The aircraft detection system was installed to avoid any risk of even slightly blinding pilots.

The laser system was installed at the 3.5 m telescope in the Spring of 1996 and in August 1996 the first LGS was created. About one year later we closed the high order AO loop while the system was locked on the LGS (section 5). Since December 1997 the LGS is increasingly reliable as the standard reference star for ALFA.

The LGS system is described in detail elsewhere in these proceedings.[4]

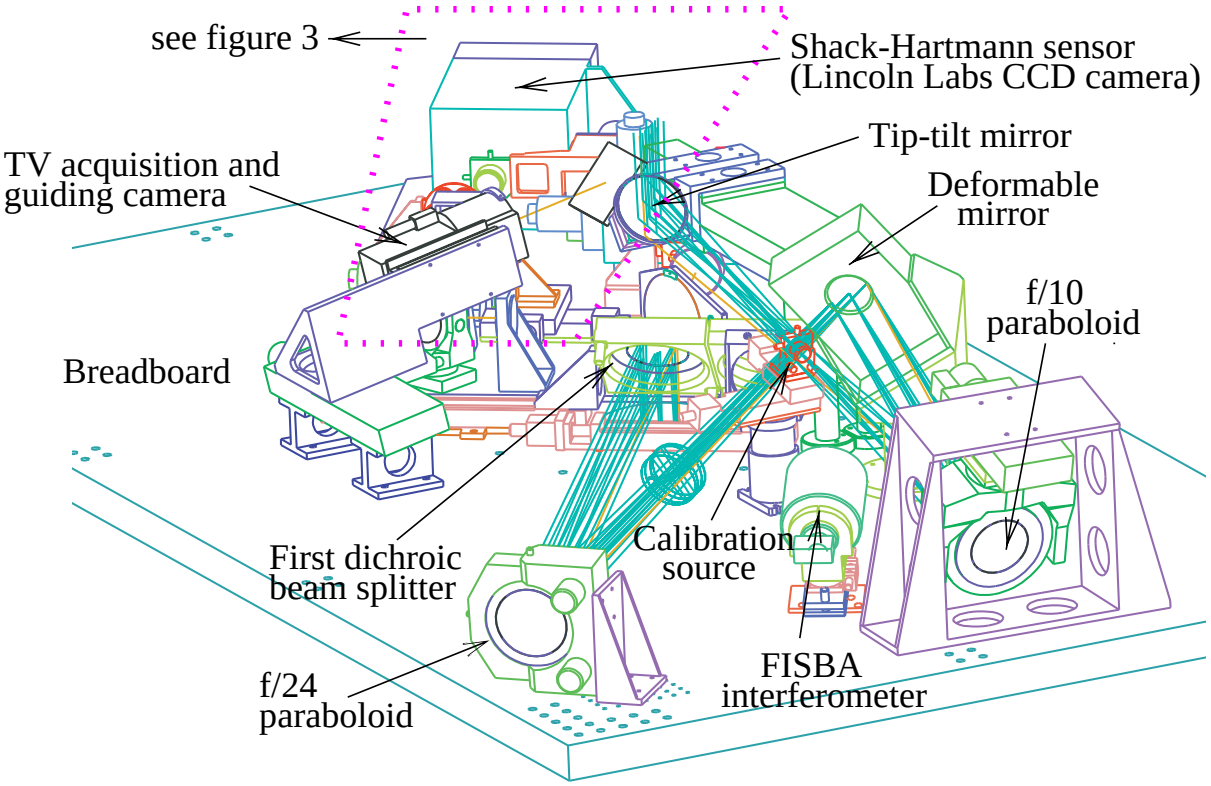

Figure 2. Right corner view of the ALFA breadboard (acquisition leg). Light from the telescope enters from top center on the drawing and hits the tip-tilt mirror. The f/10 telescope focus is in the front focal plane of the f/10 paraboloid (exactly at the position where a calibration source can be moved in). The f/10 paraboloid has a focal length of 662 mm and images the telescope pupil onto the tilted deformable mirror. After reflection at the deformable mirror the telescope focus is reimaged by the f/24 paraboloid which has a focal length of 1594 mm. The dichroic beam splitter transmits the visible light into the wave-front analyzing leg (Shack-Hartmann sensor) and reflects the infrared light into the science instrument which is mounted below the breadboard. Additionally, there is an artificial light source for optical alignment and calibration purposes, the FISBA interferometer to control the mirror surface, and a TV camera for wide field acquisition and slow scan telescope guiding.

3. THE ADAPTIVE OPTICS SYSTEM

The adaptive optics bench (Figs. 2,3) is mounted at the f/10 Cassegrain focus of the 3.5 m telescope at Calar Alto. Light coming from the secondary mirror of the telescope hits the first folding mirror of the AO system. This flat, two-axis tip-tilt mirror is used to correct the overall wave-front tip and tilt (field stabilization). This mirror is operated in closed loop mode with a bandwidth between 5–10 Hz. In natural guide star (NGS) mode, the Shack-Hartmann sensor controls this tip-tilt mirror. Using the LGS, a separate tip-tilt tracker is used for field stabilization. The tip-tilt tracker main component is a standard, slow scan CCD camera from AstroCam Ltd. in Cambridge, U.K., with a thinned EEV CCD39 chip. The 80x160 pixel CCD has a $14''$x$28''$ field of view.

The system/readout noise is about 3 electrons. The entire camera is mounted on a three-axis motorized table which permits focus adjustment and movement around the entire 180″x180″ field of view. The typical subarray size used in closed loop operation is 24 by 24 pixels binned 6 by 6 for an image with 4 by 4 pixels. Depending on the position of the subarray within the full CCD array, readout rates up to 120 Hz can be achieved. The limiting magnitude of the tracker camera under typical conditions is $m_V \approx 15$.

The two paraboloids (Fig. 2) are the main imaging elements of the optical system. The first paraboloid (f/10) images the telescope pupil onto the deformable mirror (DM) and, after the reflection at the deformable mirror, the second paraboloid (f/24) reimages the telescope focus into the science camera.

The first dichroic beam splitter reflects the infrared radiation into the science camera while the visible portion is transmitted towards the wave-front analyzing leg (AstroCam and Lincoln Labs CCD cameras, figure 3).

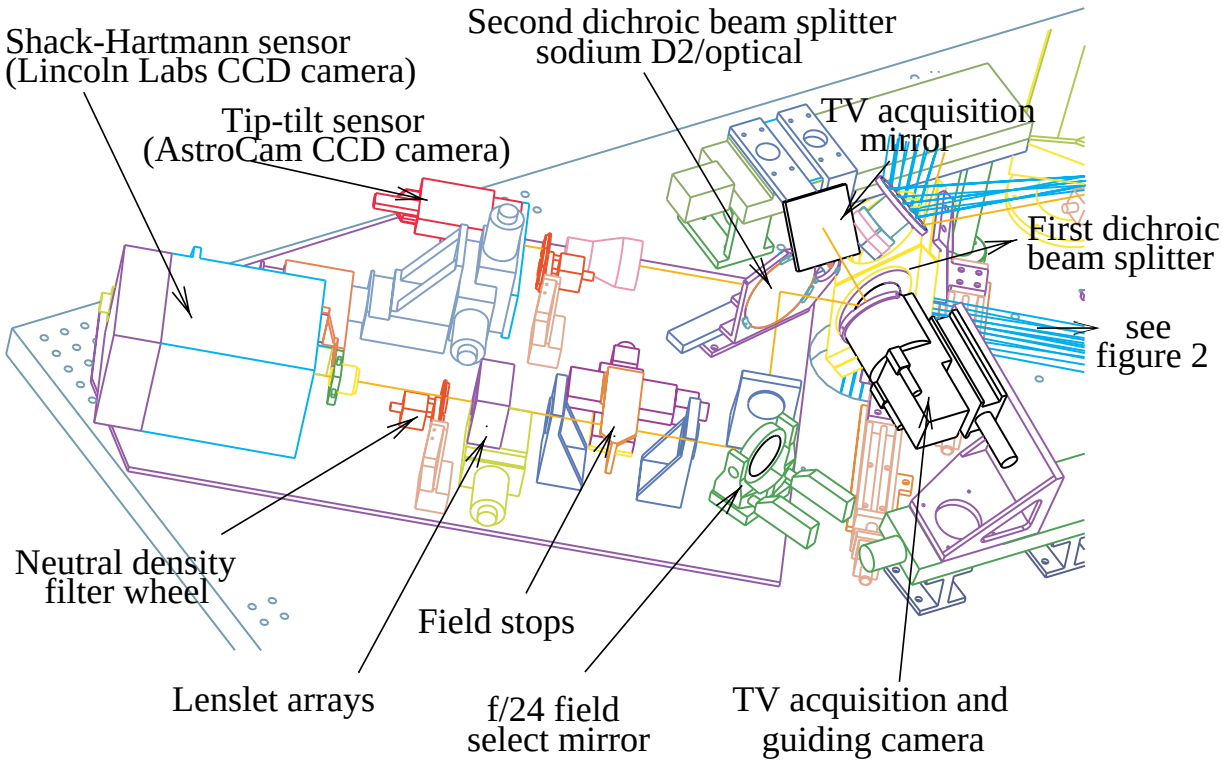

Figure 3. Left corner view of the ALFA breadboard (analyzing leg). Light from the f/24 paraboloid (figure 2) passes through the first dichroic beam splitter (science instrument/analyzing leg, figure 2) and from there through a second dichroic beam splitter to the tip-tilt sensor (AstroCam CCD camera). The sodium D_2/optical beam splitter reflects the sodium beam onto the f/24 field select mirror which is placed in reimaged pupil plane of the telescope. Tilting this mirror results in a movement of the image on the Lincoln Labs CCD camera (wave-front sensor). Between the field select mirror and the CCD camera the beam passes through a field stop (e.g. to block the Rayleigh backscatter light coming from the LGS), a lenslet array and a neutral density filter.

The deformable mirror is a standard off-the-shelf product from Xinetics Inc., U.S.A, with 97 PMN (lead magnesium niobate) ceramic actuators capable of delivering 2 µm inter-actuator stroke. After switching the power supply of the deformable mirror on and applying the same voltage to all actuators, the actuators assume slightly different lengths that have to be equalized by a special voltage per actuator pattern (*dmFlat*). Controlling this *flattening* process is accomplished by an interferometer. We use a Twyman-Green type interferometer from FISBA Optik, St. Gallen, Switzerland, which looks perpendicular onto the DM surface (Fig. 2). The rms aberration of the reflected wave is about 600 nm when the same *design null* voltage (+70V) is applied to all actuators. When the *dmFlat* pattern is applied to the DM the rms aberration goes down to 82.3 nm (Fig. 4, 0.13 λ rms = 0.13 x 632.8 nm = 82.3 nm). The peak to valley (P-V) value for the flat DM is 411 nm. Depending on the environmental temperature different *dmFlat* patterns are necessary to flatten the DM. The right panel of Fig. 4 shows the DM surface while it is correcting a trifoil-like mode.

The first optical element in the analyzing leg is either another dichroic beam splitter or a full reflective mirror. Depending on whether the system is locked on an NGS or on the LGS, either a silver coated mirror reflects the entire visible light towards the Shack-Hartmann sensor (Lincoln Labs CCD camera) or the sodium D_2/optical beam splitter reflects the Na D_2 line towards the Shack-Hartmann sensor and transmits the remaining light to the tip-tilt tracker (AstroCam CCD camera). The f/24 field select mirror in front of the Shack-Hartmann sensor is in a reimaged pupil plane. Tilting this mirror results in a movement of the Shack-Hartmann spots on the Lincoln Labs CCD. Two field stops, five lenslet arrays, and 6 neutral density filters can be inserted into the optical path between the field select mirror and the CCD camera. The current set of lenslets divides the main pupil in 3x3, 5x5, 9x9, 10x10, or 12x12 subapertures. A new set of lenslets with 3x3, 5x5, and 7x7 subapertures will be available shortly. The pixel scale of the Lincoln Labs CCD is 0.75″. The Lincoln Labs CCD camera has a thinned 64x64 pixel chip with a system noise of about 6 electroncs at 1200 Hz and of about 9 electrons at 60 Hz readout frequency. The higher readout noise at lower readout frequencies is due to the higher dark current. An upgrade of this camera will allow an operation at lower temperatures and therefore reduce the dark current and the system noise.

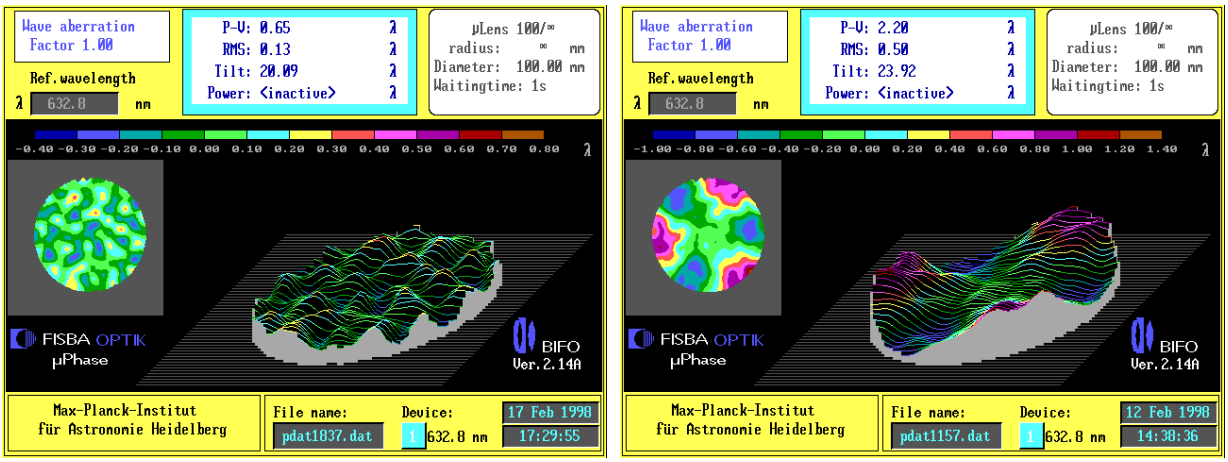

Figure 4. Interferogram of the deformable mirror in its flat position (left) and while correcting for a trifoil-like mode (right).

4. THE ADAPTIVE OPTICS CONTROL ARCHITECTURE

4.1. Data flow, hardware, software, and network

Figure 5 shows a block diagram of the ALFA network and control system architecture. The AO data flow starts at the wave-front sensor (WFS) with a maximum data rate of 9.4 MB/s. The AO data are transmitted over a fiber serial link (UFORIA: Universal Fiber Optic Repeater and Interface Assembly from AOA Inc., U.S.A.) to a VME-bus based real-time computer system running VxWorks (VME system A).

When the system is running in closed loop the reconstruction of the wave-front and the subsequent computation of the deformable mirror drive signals has to proceed as fast as possible. In closed loop operation the wave-front data are read in by one (*dataIn*) of the twenty Texas Instruments digital signal processors (DSP) of type TMS320 C40.

The AO data pipeline can be subdivided into six steps:

1. While the data are read in, *dataIn* stores the data for real-time display and transmits them over its communication channels to four additional DSP's.

2. The four *offset&gain* DSPs receive the raw data, remove all data that are not within a subaperture, calculate the background value per CCD readout channel, and perform the real-time background subtraction. In our standard setup where 18 subapertures are being processed each *offset&gain* DSP processes either 4 or 5 subapertures. Each *offset&gain* DSP feeds two *gradient* DSP's.

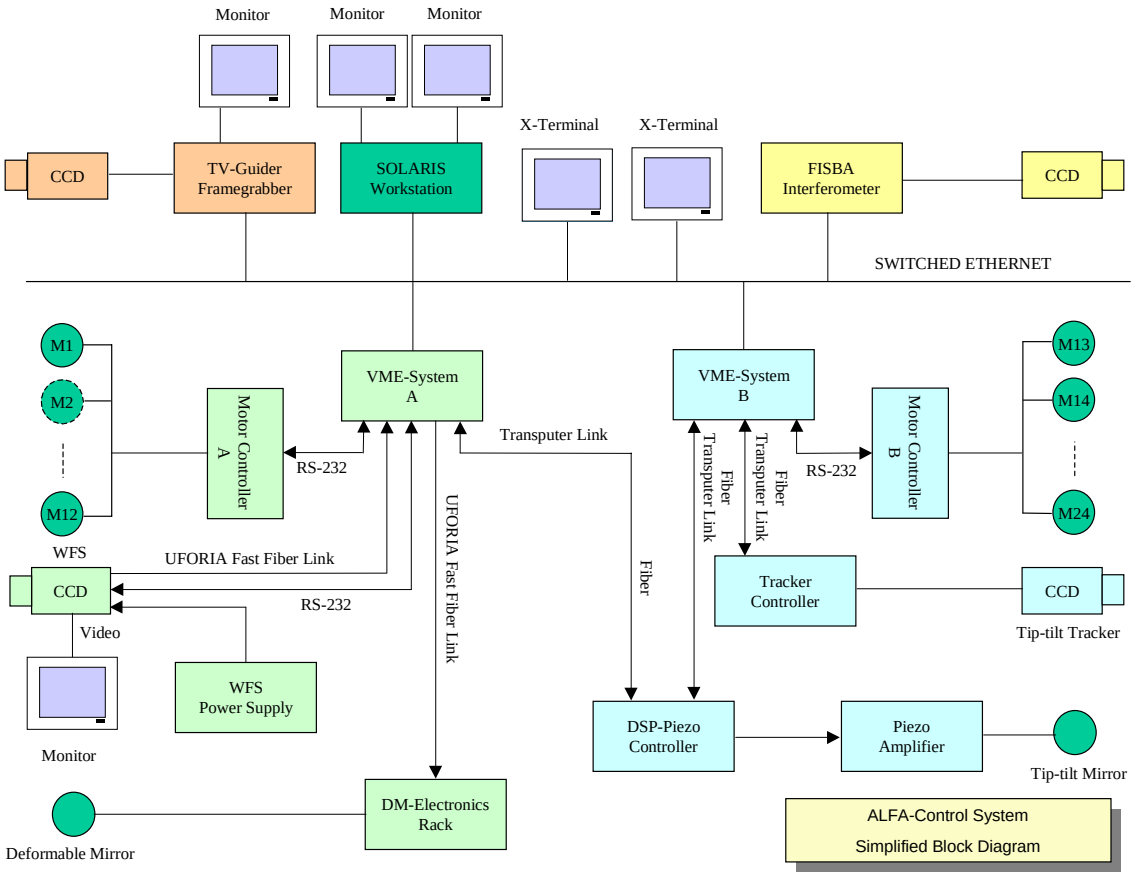

Figure 5. Block diagram of ALFA's network and control system architecture. See text in section 4.1.

3. With 18 subapertures, 6 *gradient* DSP's process 2 subapertures and 2 *gradient* DSP's process 3 subapertures. After having computed the centroid position (*centroid position* − *reference position* = *gradient*) of the guide star within a subaperture the gradients are sent to four *reconstructor* DSP's.

4. The *reconstructor* DSP's perform the wave-front reconstruction by multiplying the gradients with the reconstructor matrix (section 4.4).

5. One *compensator* DSP receives the output of the *reconstructor* DSP's, computes the uncompensated modes and performs the compensator part (PI controller or double integrator) of the control algorithm (section 4.5).

6. At the end of the AO data pipeline are two *injection* DSP's which perform the modal injection phase of the control algorithm. Compensated modes coming from *compensator* are injected into the deformable mirror actuator space and, after conversion to actuator voltages, sent over another UFORIA link to the DM electronics.

The time for an entire closed loop cycle depends on the number of subapertures, the selected centroid algorithm, and the frame-rate of the wave-front sensor. For a frame-rate of 1200 Hz, 18 subapertures, and a standard center of moment centroid algorithm, the time between start of data readout and deformable mirror update is less than 1.4 ms.

The first four steps are all synchronous and finish a few ten micro seconds after one complete wave-front image has been read in. The remaining steps 5 and 6 take typically less than 600 micro seconds thus allowing the entire control algorithm to keep up with the highest possible frame-rate of 1200 Hz (equiv. to 833 µs readout time per frame).

The DSP's are mounted in groups of four on Ariel Hydra-II boards. A Motorola 68060 CPU running VxWorks is the host for all DSP boards. This allows easy communication between graphical user interfaces (GUI) running on workstations or X-

terminals and the VME/VxWorks host.[5] The VxWorks hosts loads and controls the programs of the DSP's. The experimental physics and industrial control system EPICS*, a modern real-time database system running on top of VxWorks, reflects at any time the status of the entire system. Twelve motorized stages receive commands over a RS-232 line. A DSP-based 2-axis Piezo controller receives tip-tilt positioning commands over a 20 mega-bit/s transputer link (fiber) and steers the tip-tilt mirror in closed loop operation.

If the AO system locked on the LGS, the tip-tilt distortions calculated by the Shack-Hartmann sensor can be used to stabilize the position of the LGS on the wave front sensor. This is done by sending the tip-tilt information to another VME/VxWorks system that controls the 2-axis secondary mirror of the LGS launching telescope. The real-time database is used for this task. The tip-tilt information that is crucial for the tip-tilt correction of the observed astronomical object is sensed by a separate camera (tip-tilt tracker, section 3).

The VME/VxWorks system which controls the tip-tilt tracker (VME system B) sends tip-tilt positioning commands to the same 2-axis Piezo controller as the WFS and DM controlling VME system A. Another twelve motorized stages are controlled from this VME system.

The GUIs are written in C, Tcl/Tk, and EPICS display language DL. As an example, Fig. 6 shows the calibration GUI coded in Tcl/Tk. The implemented client/server model allows this panel being opened more than once. Pressing one of the MLM selector (lenslet array selection) buttons just sends the corresponding motor commands to the VxWorks host. The VxWorks host (server) is responsible for the proper execution.

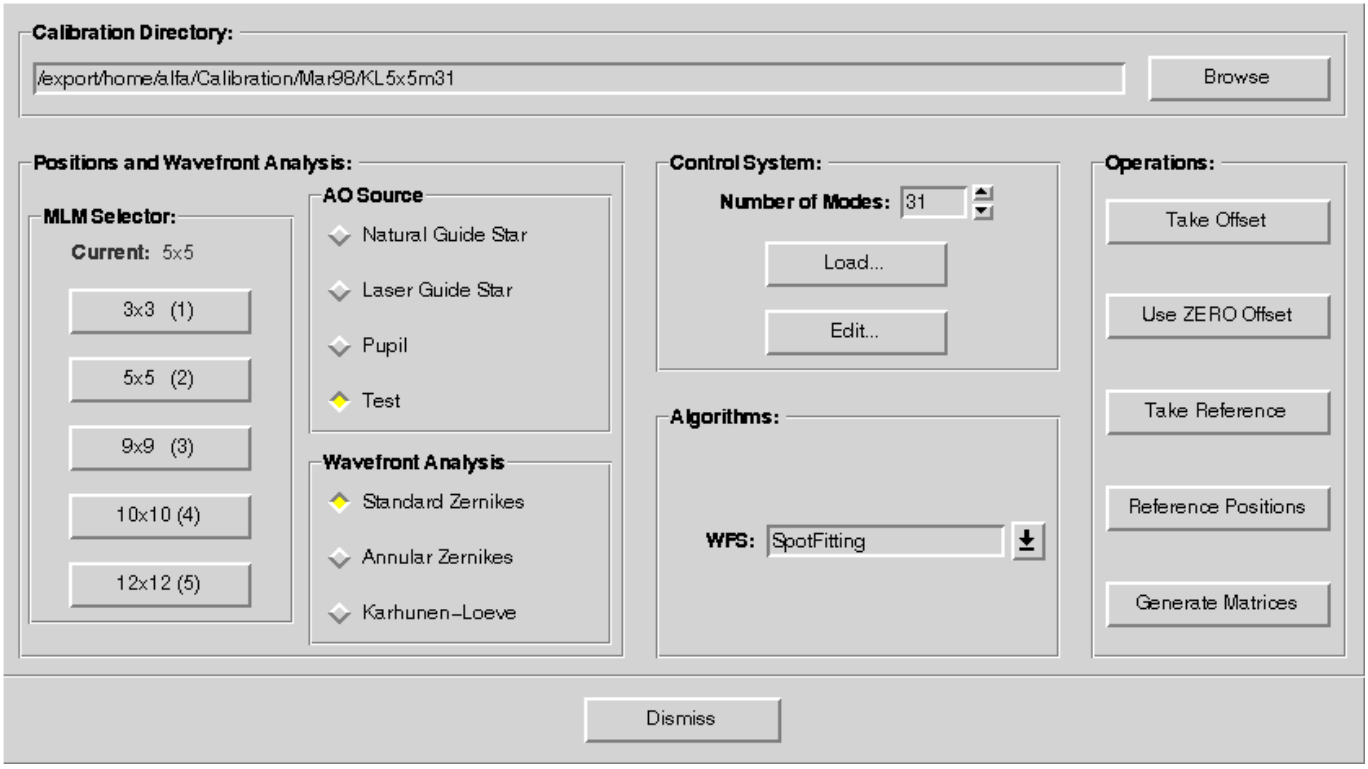

Figure 6. Calibration panel of the ALFA graphical user interface.

4.2. Control loop overview

The logical architecture employs a standard design with separate tip-tilt and deformable mirror control loops. The tip-tilt control loop was implemented using an existing tip-tilt control system developed by MPIA.[6,7] The deformable mirror control loop uses a modal compensation technique.

Several factors contributed to the selection of the modal approach for the ALFA adaptive optics system. First, it was anticipated that the coarser lenslet arrays would often be in use due to the limited available light. Only the finest lenslet array provides

*http://www.atdiv.lanl.gov/aot8/epics/Epicshm.htm

a sufficient number of gradient measurements to be able to possibly reconstruct the phase at each actuator. Second, even with the finest lenslet array, the geometry of the ALFA optical path prevents the corners of the subapertures from being aligned with the actuators. In fact, some of the actuator locations are near the center of a subaperture, which causes their effect to be almost unobservable. Also, several of the coarser arrays have hexagonal shapes that further complicate the association of corner phase values with actuators. Finally, the modal approach allows the lenslet arrays to be interchanged with a minimum of readjustments in the rest of the DM control system. Although these factors do not preclude a minimal form of zonal compensation from being implemented, the modal approach led to a simpler and more flexible design. Below we briefly describe the three basic steps of ALFA's control loop operation.[8]

4.3. Calibration

The ideal objective of the modal reconstruction operation is to determine the modal coefficients corresponding to the set of modes that are being controlled. Although it is possible to derive analytic relationships that relate the gradients to these modes and their coefficients, the relationships would be sensitive to modeling assumptions (e.g., how the gradient vectors are related to the subaperture shapes) and to the physical alignment of the subapertures and the deformable mirror. Rather than basing the modal reconstruction on an analytic model, the ALFA DM control system uses a static identification procedure to determine the effect of applying the modal injection vectors to the deformable mirror.

A reference point source is inserted into the optical path and used to illuminate the DM. Each of the modal injection vectors, i.e. the projection of the modes onto the actuator pattern, is then applied in sequence (Fig. 4 shows the DM surface when a trifoil-like mode is applied), and the static pattern of the resulting gradients is determined. These patterns are then used to compute the reconstruction matrix.

ALFA provides three different sets of modes (Standard Zernikes, Annular Zernikes[9] and the Karhunen-Loeve functions for Kolmogorov statistics[10] that can be used for the compensation. Up to now, a satisfactory flat profile of the DM (Fig. 4) was used for calibration. To remove static aberrations in ALFA's optical path, however, it is necessary to determine these aberrations, and apply offsets to the DM to compensate for them.

4.4. Reconstruction

Let $\vec{g}$ denote the resulting gradients that are recorded during calibration and $\vec{m}$ the vector of the modal coefficients. With the calibration procedure one obtains a matrix G so that $\vec{g} = G\vec{m}$. G will be left invertible if the modes that are to be controlled can be observed independently by the wave-front sensor. Assuming that this is the case, the modal coefficients can be reconstructed by building the pseudo-inverse of G, i.e. $\vec{m} = (G^t G)^{-1} G\vec{g} = Hg$, where H is called the modal reconstruction matrix.

The invisible modes which cannot be properly observed have been identified and are not used for calibration. This reduces for example the number of modes that can be used with the 5x5 lenslet array (18 subapertures) to approximately 25.

For an accurate determination of the spot centroids one can choose between three different centroiding algorithms. One does a simple weighted pixel average (WPA) using all (usually 9 by 9) pixels in the predefined subarrays of the wave-front sensor CCD. For the low signal case, another algorithm searches the brightest pixel in these arrays and uses only the surrounding 5 by 5 pixels for the WPA. The third routine fits a polynomial to the intensity distribution to determine the centroid.

4.5. Compensation

Temporal power spectra of modal coefficients[11] show that most of their energy lies at low frequencies while there is a steep decay up to high frequencies. Therefore the linear feedback design of the ALFA system attempts to attenuate the atmospheric disturbance at low frequencies at the cost of a slight amplification at high frequencies. The modal coefficients will be small if their sensitivity function (the square root of the closed loop power spectrum divided by the square root of the open loop power spectrum) is small at frequencies for which the atmospheric aberrations are large. ALFA provides two different control algorithms. One is a standard proportional-plus-integral (PI) controller and the second is an algorithm with two integrators and additional lead filtering.[12] Figure 7 shows the theoretical and experimental sensitivity functions for both controllers. As one can see, the double integrator algorithm does a good job in reducing low frequency disturbances and has a higher disturbance rejection bandwidth.

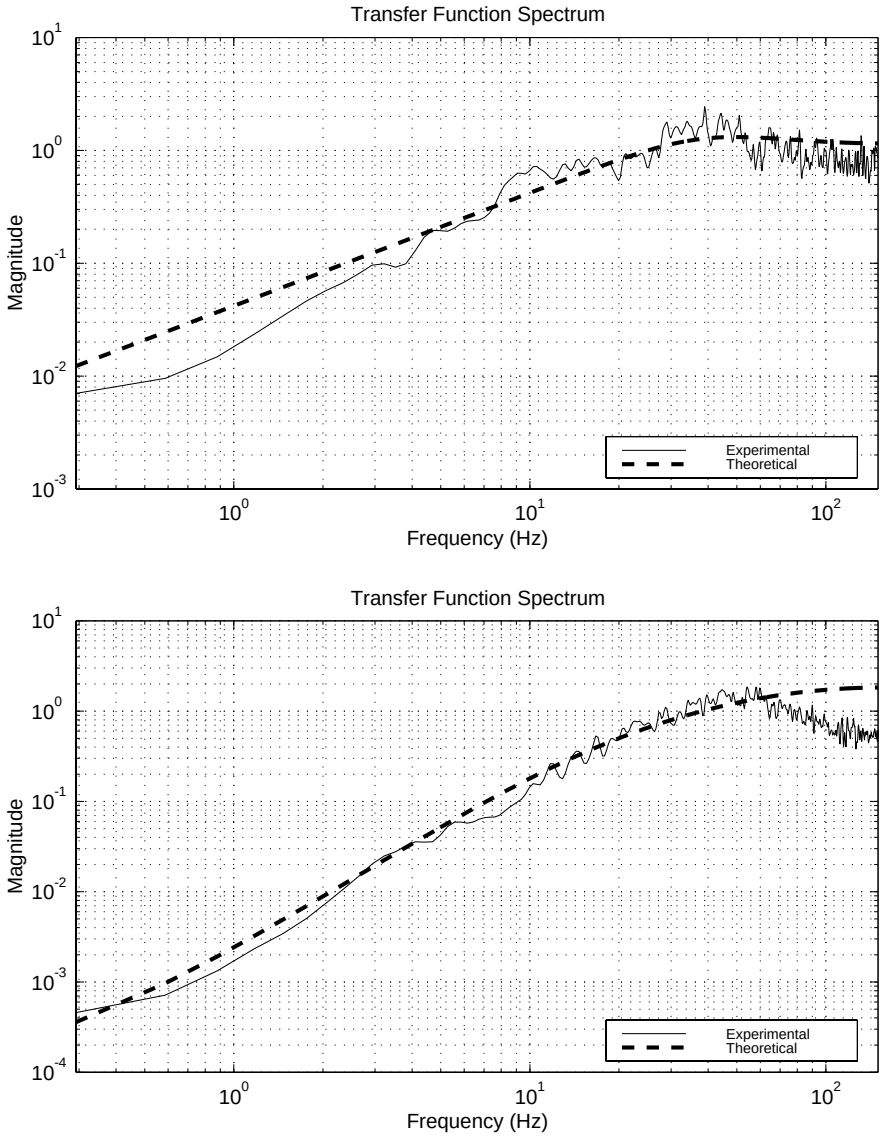

Figure 7. Sensitivity functions for two different controllers running at a loop frequency of 300 Hz. Top: proportional-integral (PI) controller giving a disturbance rejection bandwidth of approx. 25 Hz. Bottom: double integrator giving a disturbance rejection bandwidth of approx. 35 Hz. The superior performance of the experimental curves at high frequencies might be due to lower measurement errors during closed loop operation (for details see reference[12]).

5. SCIENCE CAMERA AND IMAGES

Four different science instruments have been used so far with ALFA:

- the near-infrared camera MAGIC with a 256x256 pixel detector (Rockwell NICMOS3 array) and 15″x15″field of view
- the near-infrared imaging and spectrometer instrument 3D with a 256x256 pixel detector (Rockwell NICMOS3 array), 18″x18″field of view, and a spectral resolution of 2000
- the CCD camera ALFAVIS
- the new near-infrared camera Omega Cass with a 1024x1024 pixel detector (Rockwell HAWAII array)

Omega Cass is now the primary NIR imaging camera used in conjuction with ALFA. Six wheels offer 22 filter positions, 3 pixel scales (0.12, 0.08, and 0.04″/pixel), Wollaston prisms, and various slits and grisms for low to medium resolution spectroscopy. Sub-array readout permits very short integrations for speckle observations.

The large size of the array is advantageous because in many cases the field of view contains reference stars for post-processing deconvolution (smaller arrays require a telescope slew to the reference source). Coronagraphic focal plane masks and a pupil plane Lyot stop to suppress diffraction spikes are being implemented and tested.

Table 1 summarizes the performance of ALFA during the 1997-1998 observing season using both natural and laser guide stars under different intrinsic seeing conditions. Closed loop AO operation (60 Hz, 9 modes) is possible for natural guide stars as faint as V = 12 mag under sub-arcsecond conditions, as well as the LGS at V = 10 mag.

ALFA currently provides strehl ratios near 10% using natural guide stars brighter than V = 9 mag, and 2-4% with the LGS. Our first closed loop operation on an LGS and a science target is shown in Fig. 8. The V = 9 mag components of the binary BD +31°643 have 0.6″ separation and are unresolved in 1 second integrations at K and with tip-tilt correction only. Higher order AO with the LGS (60 Hz, 7 modes & tip-tilt) provides resolved images of the binary.

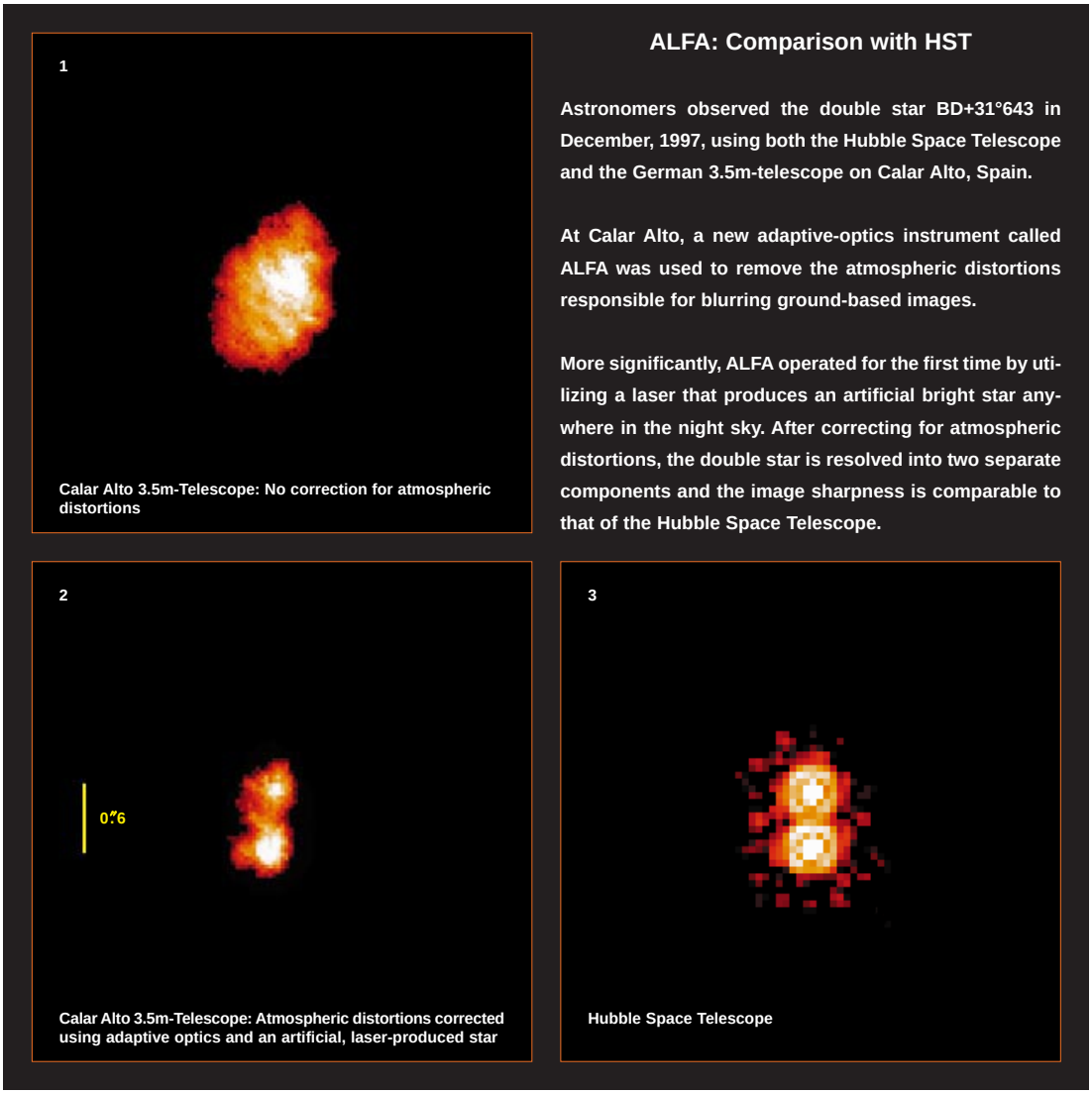

Figure 8. Press release reporting our first successful image improvement using ALFA locked on the LGS. Data were obtained in K-band using Omega Cass.

K-band images of the Orion Trapezium contain stars in the entire 80"x80" field of view of the detector. We found that the best corrected stellar images (FWHM's = 0.2″) lie within 15″ radius of the natural guide star (θ^1 Ori C), whereas at the outskirts of the detector we measure FWHM's = 0.4″. Intrinsic seeing is roughly 0.6″. Our group's main science interest in Orion is to constrain the binary frequency in this star forming region, as well as to study the arcsecond scale proplyds discovered in HST optical images. Despite the large number of bright stars in the Orion nebula that could be used as natural guide stars, most science targets do not lie within the sub-arcminute isoplanatic patch suggested by our measurements. Optimization of the laser as a wave-front reference therefore appears imperative for obtaining fully corrected images of our science objects.

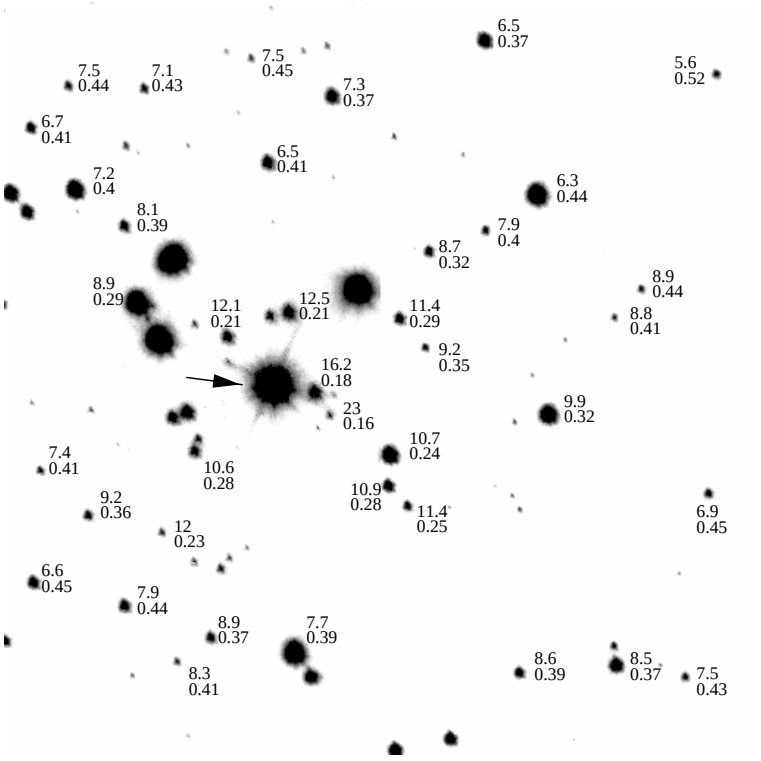

Figure 9. K-band image of the Orion Trapezium. Field of view is 80″x80″. ALFA was locked on θ^1 Ori C (arrow). The pairs of numbers give the Strehl number (upper) and FWHM in arcsec (lower) of the corresponding object.

6. CONCLUSIONS AND OUTLOOK

After one and a half year of observing with ALFA, there is still much work to be accomplished. ALFA is (still) not a turn-key instrument. Therefore the astronomers will have support by a specialized night assistant (ALFA operator).

Communication among the various instruments (telescope, science camera, TV-guider, LGS and the AO part of ALFA) has to be modified such that macro procedures can control one entire observing sequence, including mosaicing techniques. For 1998 we have planned to install a new, better cooled Shack-Hartmann sensor and a new DM control electronics. An APD quad-cell detector for tip-tilt measurements is foreseen for 1999.

ACKNOWLEDGEMENTS

We thank our colleagues at MPE and on Calar Alto for their collaboration on the ALFA project. We would also like to acknowledge the adaptive optics group of Adaptive Optics Associates Inc., Massachusetts, U.S.A: Allan Wirth, Joseph Navetta, Carlos Caicedo, Stacy Kahalas, Andrew Jankevics, Frank Landers, Fred Huettig, Theresa Bruno, and Lawrence Schmutz.

REFERENCES

1. A. Glindemann, D. Hamilton, S. Hippler, R.-R. Rohloff, and K. Wagner, "Alfa – the laser guide star adaptive optics system for the calar alto 3.5-m telescope," in *Laser Technology for Laser Guide Star Adaptive Optics Astronomy*, N. Hubin, ed., pp. 120–125, European Southern Observatory, (Garching, Germany), 1997.

Guide star	Seeing [arcsec]	No. of Subap-ertures	Loop band-width [Hz]	Corrected FWHM [arcsec]	Corrected Strehl [%]	Loop robust-ness	WFS signal/ noise
Bright NGS	1.3-1.8	18	90	≤0.3	≈10	++	>100
$m_V \approx 5$	0.9-1.2	18	90	≤0.3	≈20	++	>100
Faint NGS	1.3-1.8	6 or 18	10	≤0.3	5-10	+	10-20
$m_V \approx 10$	0.9-1.2	18	20	≤0.3	5-10	++	10-20
Very faint	1.3-1.8	6	6	?	?	+-	≤5
NGS $m_V \approx 12$	0.9-1.2	6	6	0.7	3	+	≤5
LGS	1.3-1.8	6	6	≤0.5	2–3	+-	≤5
$m_V \approx 10$	0.9-1.2	6 or 18	6-10	≤0.4	≈4	+	≤5
Lick LGS $m_V=7$	0.8	37	30	0.3	9.1	?	?
ESO ADONIS $m_V=12$	< 1	32	10	0.3	9	++	?

Table 1. ALFA performance in K-band vs. seeing and reference star brightness. NGS: Natural guide star. LGS: Laser guide star. Lick observatory data from reference.[13] ESO data from reference[14] and private communication.

2. A. Quirrenbach, W. Hackenberg, H.-C. Holstenberg, and N. Wilnhammer, "The alfa dye laser system," in *Laser Technology for Laser Guide Star Adaptive Optics Astronomy*, N. Hubin, ed., pp. 126–131, European Southern Observatory, (Garching, Germany), 1997.
3. A. Quirrenbach, W. Hackenberg, H.-C. Holstenberg, and N. Wilnhammer, "The sodium laser guide star system of alfa," in *Adaptive Optics and Applications*, R. K. Tyson and R. Q. Fugate, eds., *Proc. SPIE* **3126**, pp. 35–43, 1997.
4. R. Davies, W. Hackenberg, T. Ott, A. Eckart, H.-C. Holstenberg, S. Rabien, A. Quirrenbach, and M. Kasper, "Alfa: First operational experience of the mpe/mpia laser guide star system for adaptive optics," in *Adaptive Optical System Technologies*, R. Tyson and R. Fugate, eds., *Proc. SPIE* **3353**, p. Paper 94, 1998.
5. A. Wirth, J. Navetta, and B. M. Levine, "Real-time modal control implementation for adaptive optics," in *Optical Telescopes of Today and Tomorrow*, A. L. Ardeberg, ed., *Proc. SPIE* **2871**, pp. 871–877, 1997.
6. A. Glindemann, "Relevant parameters for tip-tilt systems on large telescopes," *Publ. Astron. Soc. Pac.* **109**, pp. 682–687, 1997.
7. A. Glindemann, M. McCaughrean, S. Hippler, C. Birk, K. Wagner, and R.-R. Rohloff, "Charm - a tip-tilt tertiary system for the calar alto 3.5 m-telescope," *Publ. Astron. Soc. Pac.* **109**, pp. 688–696, 1997.
8. A. Wirth, J. Navetta, D. Looze, S. Hippler, A. Glindemann, and D. Hamilton, "Real-time modal control implementation for adaptive optics," *J. Opt. Soc. Am.* **to appear**, 1998.
9. V. N. Mahajan, "Zernike annular polynomials and optical aberrations of systems with annular pupils," *Eng. & Lab Notes, in Opt. & Phot. News* **5**, pp. 8125–8127, 1994.
10. R. C. Cannon, "Optimal basis functions for wave front reconstruction and simulation," *J. Opt. Soc. Am.* **submitted**, 1996.
11. A. Glindemann, "Beating the seeing-limit," Habilitationsschrift, Univ. Heidelberg, 1997.
12. D. Looze, M. Kasper, S. Hippler, and O. Beker, "Analysis of effective measurement errors for shack-hartmann sensors in closed-loop adaptive optics operation," **in preparation**.
13. C. Max, S. Olivier, H. Friedman, J. An, K. Avicola, B. Beeman, H. Bissinger, J. Brase, G. Ebert, D. Gavel, K. Kanz, M. Liu, B. Macintosh, K. Neeb, J. Patience, and K. Waltjen, "Image improvement from a sodium-layer laser guide star adaptive optics system," *Science* **277**, pp. 1649–1652, 1997.
14. D. Bonaccini, E. Prieto, P. Corporon, J. Christou, D. L. Mignan, P. Prado, and N. Hubin, "Performance of the eso ao system, adonis, at la silla 3.6 m telescope," in *Adaptive Optics and Applications*, R. Tyson and R. Fugate, eds., *Proc. SPIE* **3126**, pp. 589–594, 1997.